

Experimental Study on Shear Mechanical Properties and Section Morphology of Coal Samples

Sihao Huang, Tingkan Lu, Baohua Guo

School of Energy Science and Engineering, Henan Polytechnic University, Jiaozuo, China

Email: 18768980127@163.com

How to cite this paper: Huang, S.H., Lu, T.K. and Guo, B.H. (2023) Experimental Study on Shear Mechanical Properties and Section Morphology of Coal Samples. *World Journal of Engineering and Technology*, 11, 335-352.

<https://doi.org/10.4236/wjet.2023.112024>

Received: April 9, 2023

Accepted: May 19, 2023

Published: May 22, 2023

Copyright © 2023 by author(s) and Scientific Research Publishing Inc.

This work is licensed under the Creative Commons Attribution International License (CC BY 4.0).

<http://creativecommons.org/licenses/by/4.0/>



Open Access

Abstract

The mechanical properties of rocks under cyclic and dynamic loading are important research topics for solving the structural stability of large engineering rocks. As underground mining in coal mines goes deeper, ground stresses are increasing and instability damage of coal rocks by shear loading is frequent. Therefore, in order to investigate the shear mechanical properties and section morphological characteristics of intact coal samples in the direct shear test, the RDS-200 rock direct shear instrument was used to carry out direct shear tests on intact coal samples under different normal stresses, and the shear section was scanned for three-dimensional morphology. The results show that: 1) from the strength characteristics, the peak shear strength of the coal samples increased linearly with increasing normal stress, and the residual shear strength increased logarithmically. 2) In terms of deformation characteristics, the peak shear displacement of the coal sample increases linearly with increasing normal stress, the pre-peak shear stiffness increases logarithmically, and the residual normal displacement decreases linearly. 3) From the morphological characteristics of the shear surface, with the increase of normal stress, the section transitions from high-order undulating to flattening type. The maximum height of the fracture surface profile and kurtosis coefficient of the shear section decreased linearly, and the profile area ratio and root mean square of slope decreased as a power function, *i.e.* the higher the normal stress, the smaller the undulation of the section, the sharpness of the roughness shape and the roughness coefficient JRC, and the flatter and smoother the section. The findings of this study can help to provide some reference for the evaluation of shear instability occurring in coal bodies under different normal stresses.

Keywords

Coal, Shear Test, Normal Stress, Shear Section, Three-Dimensional

1. Introduction

One of the main forms of damage to a rock body is through-joint damage due to shear loading, such as landslides, fracture tectonic earthquakes, and high level collapse of mountains [1]. In mining rock mechanics, the shear resistance of the coal body is also important, as it is affected by the shear capacity of the coal rock itself when sliding along a large structural surface of a fault or when sliding of the coal block from the excavation boundary [2]. Therefore, it is important to carry out experimental research on the effects of different normal stresses on the shear mechanical properties and shear surface morphology of coal samples under shear loading, in order to control the stability of the roadway surrounding rock and achieve safe mine production.

2. Review of the Literature

2.1. Study of Shear Mechanical Properties of Rocks

In recent years, many scholars at home and abroad have conducted a large number of experimental and theoretical studies on the shear mechanical properties of coal rock bodies and the morphological characteristics of jointed surfaces. In terms of shear mechanical properties of coal rock, Li [3] conducted a shear creep test study on weak structural surfaces of sandstone with different water contents, and the results showed that the creep deformation of the weak structural surfaces of sandstone in a watery state compared with a dry state had a large difference, and the water in the structural surfaces would weaken the shear strength of the weak structural surfaces of sandstone due to the softening and lubricating effects. Li [4] used artificial casting to produce regular serrated joint faces for direct shear test research, and the results showed that the greater the shear rate, the lower the shear strength of the rock; the greater the undulation angle of the joint face, the higher the shear strength of the rock. Wang [5] conducted a direct shear test study on red sandstone with different water contents and explored the relationship between the shear characteristics of red sandstone and the water content of the sandstone. Xiao [6] conducted shear tests on coal samples using a variable angle shear mould and an acoustic emission system, and the results showed that the shear angle showed a negative correlation with the positive stress, shear stress, peak load and stiffness. Peng [7] carried out a fine shear test on gas-bearing coal rocks using a self-developed shear test device, and analysed the fractal characteristics of the crack distribution in the shear-broken section. Xu [8] used a self-developed coal rock shear-percolation coupling test apparatus to conduct a shear-percolation coupling test on coal under different normal stresses. Wang [9] conducted shear tests on rough rock joints at different shear rates and found that the peak shear strength of the joints decreased with increasing shear rate, and proposed a shear strength model for

rough joints considering shear rate. Li [10] investigated the shear behaviour of the natural coal-rock interface by conducting indoor direct shear tests on coal-rock specimens under constant normal stress conditions.

2.2. Study on the Morphology of Structural Plane

In terms of the morphological characteristics of coal rock joints, Xu [11] carried out indoor shear tests and 3D scanning of sections on sandstone and explored the morphological characteristics of sandstone shear sections. Xia [12] [13] [14] studied a 3D rock morphology scanning device, developed a portable 3D rock morphology scanner, and developed a calculation program for morphology information. Jiang [15] used the Gaussian filter method to study the variation of joint surface morphology under shear loading. Fan [16] conducted multiple shear tests on the same joint surface using different normal stresses. The study showed that the complexity of the joint surface morphology decreased under multiple shear effects, but the effect on the anisotropic nature of the joint surface was relatively small. Liu [17] used the two-dimensional joint profile measured by the measurement method to reconstruct the three-dimensional morphology of rock joints. Huang [18] proposes a visualisation method for tracking the surface morphology of joints, which can accurately describe the total shear area at different shear stages.

2.3. Problems and Summary

In summary, some results have been achieved in the study of the shear mechanical properties and morphological characteristics of rock joints at this stage, with most of the research results coming from rocks and coal, and relatively little research has been carried out on the shear mechanical properties and section morphological characteristics of raw coal under different normal stresses. In addition, the shear mechanical properties of coal rocks are usually studied by means of artificially prefabricated through joints, which are still different from the mechanical and morphological characteristics of natural non-through joints in coal rocks subjected to compressive shear loads. Therefore, this paper proposes to carry out a direct shear test study of intact coal samples under different normal stresses, and to carry out a three-dimensional morphological scan of the shear section to analyse the effect of the normal stress on the shear mechanical and morphological parameters of the coal samples.

3. Test Overview

3.1. Sample Preparation

The coal samples used in the tests were taken from the Zhongma Village coal mine in Jiaozuo City, Henan Province, where the coal was mostly brownish-black in colour and the coal seams were fissured. All coal samples used in the tests were taken from the same batch of mining, and coal samples were processed from the test coal blocks using a rock corer, an automatic rock cutting machine

and an automatic rock double-sided grinder equipment. A standard cylindrical specimen of $\Phi 50 \text{ mm} \times 100 \text{ mm}$ was processed by the drilling, sawing and grinding processes, as shown in **Figure 1**.

Uniaxial, triaxial and Brazilian splitting tests were carried out on complete standard cylindrical specimens using the RMT-150B rock mechanics servo tester developed by the Wuhan Institute of Geotechnics, Chinese Academy of Sciences, and the basic mechanical property parameters of the specimens were obtained as shown in **Table 1**.

3.2. Test Equipment

The shear test system RDS-200, designed by GCTS, USA, was used to perform the coal sample straight shear test, which has the advantages of high accuracy, easy operation and simple programming of the test procedure. The test set-up is shown in **Figure 2**. The shear actuator and normal actuator are capable of providing a load of 10 t and 5 t respectively, with a shear stroke of 25 mm and a normal stroke of 24 mm. a simplified diagram of the shear area is shown in **Figure 3** below.

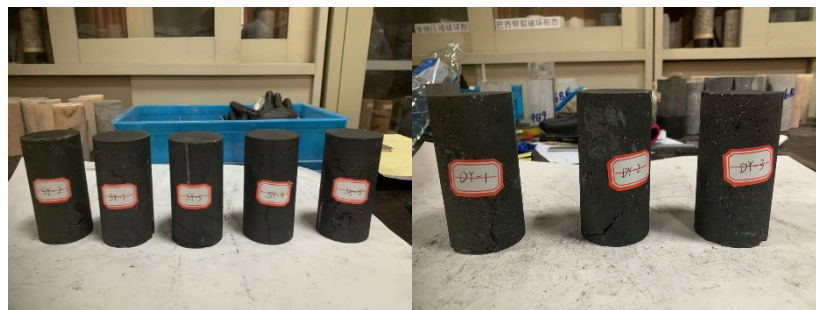


Figure 1. Part of a complete specimen.

Table 1. Table type styles (Table caption is indispensable).

Sample type	σ_c (MPa)	σ_t (MPa)	E (GPa)	μ	φ ($^\circ$)	C (MPa)
Coal	12.52	0.31	4.52	0.57	47.8 $^\circ$	4.65

In the table, σ_c is the compressive strength, σ_t is the tensile strength, μ is the Poisson's ratio, E is the modulus of elasticity, φ is the angle of internal friction, and C is the cohesive force.

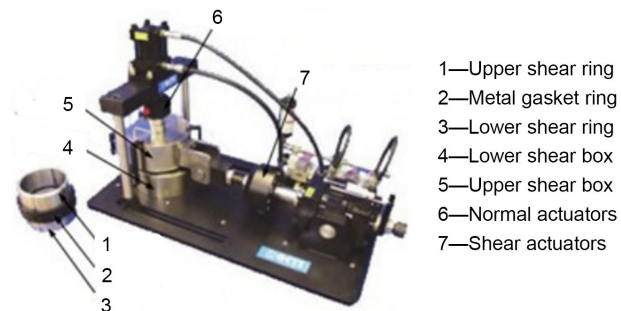


Figure 2. RDS-200 straight shear test system.

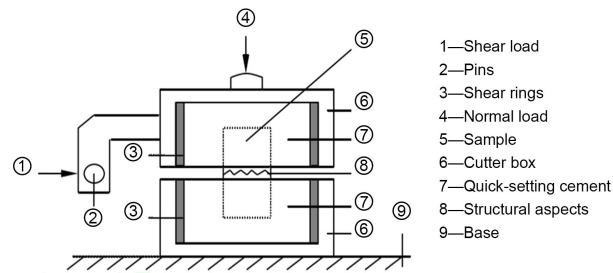


Figure 3. Simplified diagram of shear area.

3.3. Cross-Sectional 3D Morphology Parameter Acquisition

The OKIO-400 laser scanner (**Figure 4**) jointly developed by Beijing Tianyuan 3D Technology Co., Ltd. and Tsinghua University was used to scan the three-dimensional shape of the shear surface, with a measurement range of 400×300 mm - 200×150 mm, measurement accuracy of 0.03 mm - 0.02 mm, average point distance of 0.31 mm - 0.15 mm, scanning method of non-contact surface scanning, stitching method of fully automatic marker point. The accuracy control method is GREC global error control module.

3.4. Test Programme and Procedures

The specimens need to be encapsulated before the test starts, and the encapsulation of the specimens is crucial to the smooth running of the straight shear test and the accuracy of the test results. The specimen encapsulation process is shown in **Figure 5** below.

Lower shear ring encapsulation (a-c): first in the silicone mould poured cement pad, pad in the lower side of the specimen placed in the middle, the purpose is to control the shear fissure surface appears in the middle of the specimen; two shear ring should be coated with a layer of butter inside it, to facilitate demoulding; then the quick-setting cement at 1:4 water-cement ratio mixed evenly and injected into the lower shear ring, cement slurry added to the top of the shear ring parallel to it, wait for the quick-setting Wait for the cement to set and complete the encapsulation of the lower shear ring.

The upper shear ring is encapsulated (d-g); a layer of rubber cement is placed on the surface of the solidified cement block in the lower shear ring, the purpose of which is to isolate the cement from the upper and lower shear rings; a metal gasket ring is placed on the lower shear ring to provide a suitable space for the shearing process; the upper shear ring is placed on the metal gasket ring and the gap between the upper and lower shear rings is sealed with rubber cement to prevent the cement liquid from leaking out; after which the rapid setting cement continues to be poured in the upper shear ring Afterwards, the cement is poured into the upper shear ring until the cement level is parallel to the upper shear ring and the cement sets.

Place in the shear box (h-i): after the cement has set, place the finished specimen in the lower shear box, align the upper shear box, fix the bolts and set up the test program on the GCTS system computer to start the straight shear test.

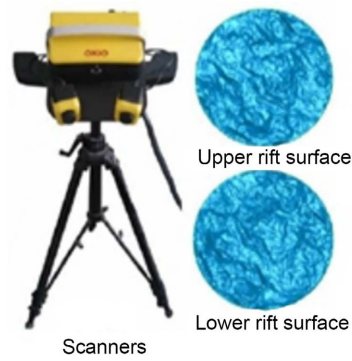


Figure 4. OKIO-400 laser scanner (left), 3D model of nodal surface (right).

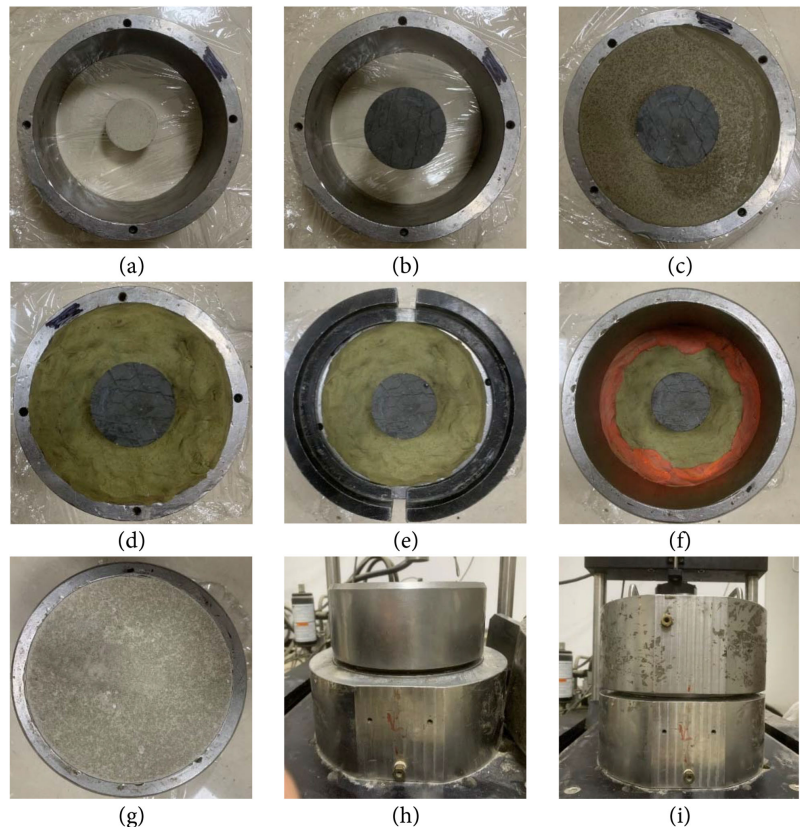


Figure 5. Specimen encapsulation process.

The shear tests are conducted under normal stress (CNL) conditions with design values of normal stress of 0.5 MPa, 1 MPa, 1.5 MPa, 2 MPa and 2.5 MPa:

- 1) Apply the normal stress to the design value in a load-controlled manner;
- 2) Application of tangential load in a displacement-controlled manner with a shear rate of 1 mm/min;
- 3) The normal stress is kept constant during shear and the straight shear test is terminated when the shear displacement reaches 10 mm;
- 4) At the end of the straight shear test, the specimen is removed from the press and the sample is taken out of the press and scanned using a three-dimensional

profile scanner with marker points.

4. Straight Shear Test Results and Analysis

4.1. Strength Characteristics

The strength characteristics of the coal samples under different normal stresses are shown in **Figures 6-8**. **Figure 6** shows the shear stress-shear displacement curves of the coal samples at different normal stresses, **Figure 7** shows the fitted relationship between the peak shear strength and the normal stress of the coal samples, and **Figure 8** gives the relationship between the shear strength value (hereafter referred to as the residual shear strength) and the normal stress of the coal samples at a shear displacement of 10 mm.

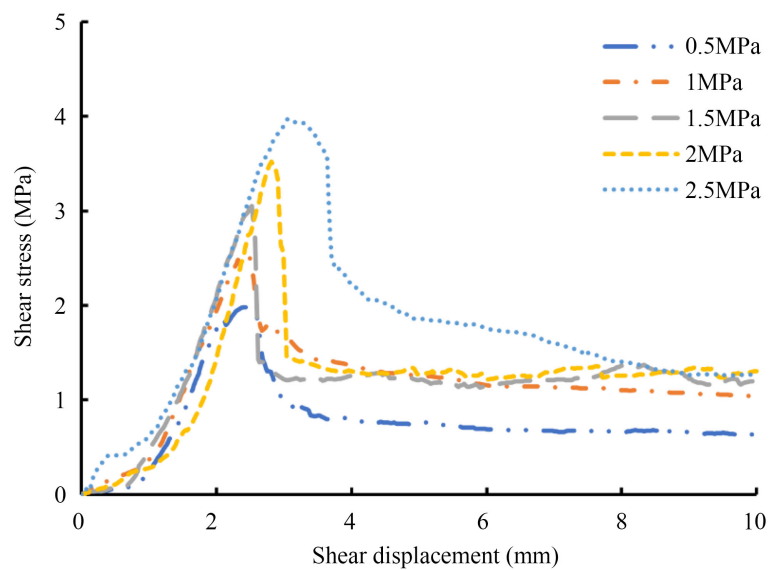


Figure 6. Shear stress-shear displacement curves for coal samples.

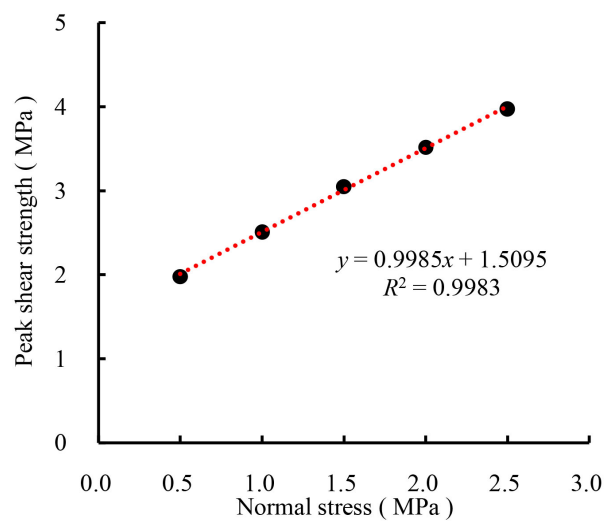


Figure 7. Relationship between peak shear strength and normal stress.

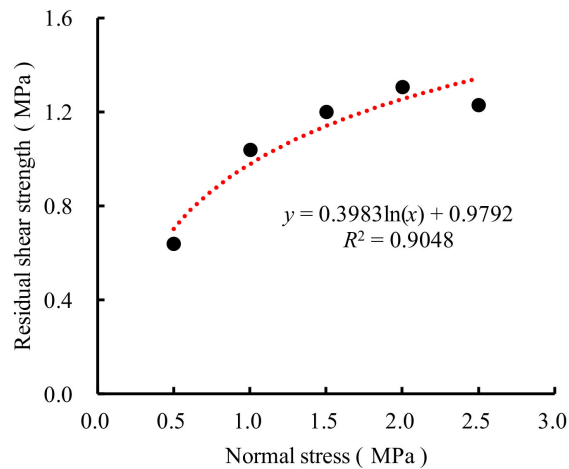


Figure 8. Relationship between residual shear strength and normal stress.

As can be seen from **Figure 6**, the shear stress-shear displacement curve of the coal sample can be roughly divided into five stages: 1) Initial compacting stage. The curve at this stage is slightly convex downwards, the fracture pores inside the coal sample are compacted, the primary microfractures are gradually closed and the specimen is gradually compacted. It is worth noting that the coal sample is not homogeneous and some of the internal primary microfracture pores are more numerous and experience a longer time at this stage. 2) Linear stage. As the test proceeds, when the shear force increases to a certain value, it enters the linear stage, the curve at this stage is nearly straight, the shear stiffness is almost constant, and the shear stress increases rapidly with the increase in shear displacement. 3) Yield stage. Mechanical properties from the elastic to plastic, the coal sample internal shear stress due to the role of micro-fractures, and gradually formed a local fracture, with the shear stress reaches the peak, the coal sample internal local fractures continue to develop and expand, accompanied by a "thunk" sound, the formation of penetration near the intended shear surface. 4) Softening stage. At this point, the shear stress falls rapidly, the projection of the shear surface is gradually cut off, and the overall roughness of the shear surface gradually decreases. 5) Residual stage. The curve at this stage is approximately horizontal, and the shear stress value does not drop significantly.

From the above variation characteristics of shear stress, the shear strength characteristics of coal samples have a certain relationship with the magnitude of normal stress. From **Figure 7**, **Figure 8**, it can be seen that the peak shear strength of the coal sample increases with the increase of the normal stress in a good linear relationship, and the goodness of fit R^2 value reaches 0.99. The residual shear strength of the coal sample increases approximately as a logarithmic function of the normal stress, and the goodness of fit R^2 value reaches 0.90. In the residual stage, the tiny convex body of the coal sample section is ground flat under the normal stress, and the curve is approximately horizontal. The higher the normal stress, the greater the friction generated by the closer contact be-

tween the sections and the greater the residual shear strength.

4.2. Deformation Characteristics

The deformation characteristics of the coal samples under different normal stresses are shown in **Figures 9-12**. The normal displacement-shear displacement curves of the coal samples are shown in **Figure 8**, where the negative values of the vertical coordinates indicate shear contraction and the positive values indicate shear expansion. **Figure 10** shows the shear displacement at the peak shear strength of the coal sample (hereafter referred to as the pre-peak shear stiffness) versus the normal stress. **Figure 11** shows the slope of the curve at the point where the shear stress is equal to 50% of the peak shear strength (hereafter referred to as the pre-peak shear stiffness) versus the normal stress. **Figure 12** shows the normal displacement of the coal sample at a shear displacement of 10 mm (hereinafter referred to as the residual normal displacement) versus the normal stress.

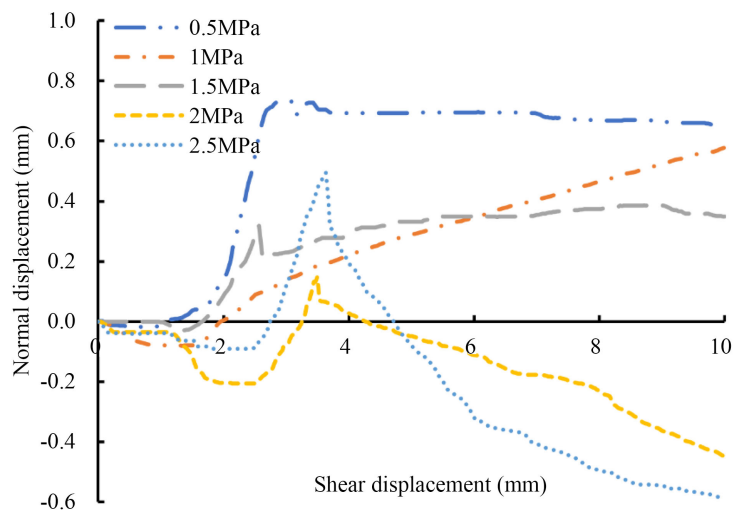


Figure 9. Normal displacement-shear displacement curves for coal samples.

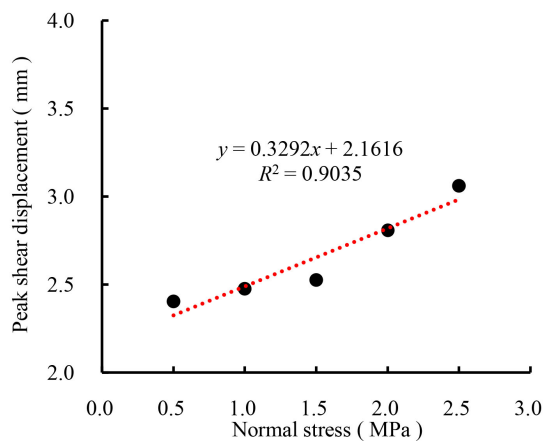


Figure 10. Relationship between peak shear displacement and normal stress.

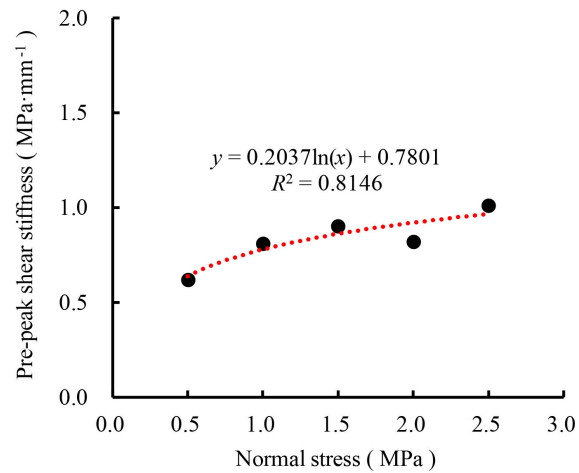


Figure 11. Relationship between pre-peak shear stiffness and normal stress.

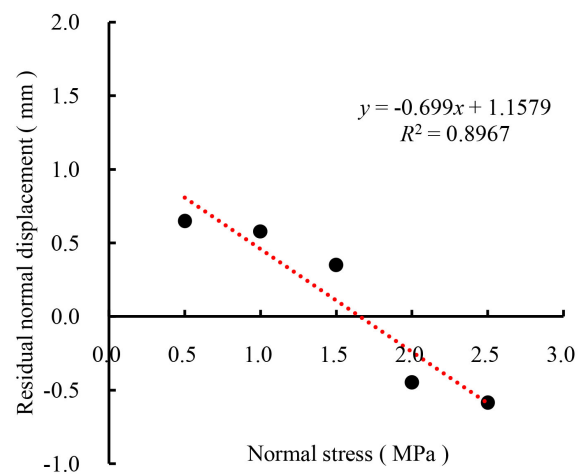


Figure 12. Relationship between residual normal displacement and normal stress.

As can be seen from **Figure 9**, the normal displacement-shear displacement curves all show a relatively slight trend of shear contraction followed by shear expansion in the initial stages. 1.5 MPa, 2 MPa and 2.5 MPa normal stresses show an obvious phenomenon of normal shear expansion before normal shear contraction near the peak shear displacement, while this phenomenon is not obvious at 0.5 MPa and 1 MPa, which is due to the fact that the irregular micro-convexity of the shear surface is heavily crushed from the root and the stripping of the joints is misaligned under the higher normal stress. This is due to the large number of irregular micro-convex bodies in the shear surface being crushed from the roots and the stripping misalignment of the joint surface under the action of higher normal stresses. In general, the shear swelling effect of the samples is related to the normal stress, with the deformation characteristics of the samples exhibiting normal shear swelling after shearing at low normal stresses, while at high normal stresses, the shear swelling effect is limited and the samples exhi-

bit normal shear shrinkage after shearing.

As can be seen from **Figure 10**, the peak shear displacement of the coal sample tends to increase linearly with increasing normal stress. The distribution of peak shear displacement ranged from 2.4 mm to 3.1 mm. For the peak shear displacement, Barton [19] considered the Joint Roughness Coefficient (*JRC*) as the main factor affecting the peak shear displacement and proposed an empirical equation to predict the peak shear displacement, while Wibowo [20] considered the normal load as the main factor affecting the peak shear displacement. Asadollahi [21] argued that *JRC* and normal stress jointly influenced peak shear displacement, and that peak shear displacement was positively related to normal stress and negatively related to *JRC*. In this paper, there is no prefabricated joint surface, so the roughness coefficient *JRC* of the joint surface before shearing is not known, but from the test results, the fitted curves of peak shear displacement and normal stress are highly linearly correlated, and the R^2 value of the goodness of fit is 0.90, indicating that normal stress is the main influencing factor of peak shear displacement.

From **Figure 11**, it can be seen that the peak front shear stiffness of the coal sample increases with increasing normal stress in a roughly logarithmic relationship, with a goodness of fit R^2 value of 0.81. The higher the normal stress, the flatter the trend of increasing peak front shear stiffness. The data points fluctuate, possibly due to the inhomogeneity of the coal sample.

As can be seen from **Figure 12**, the residual normal displacement and the normal stress in general tend to decrease roughly linearly, the higher the normal stress, the shear surface climbing shear expansion effect is limited and the section projection is transformed from tip damage to root, thus leading to the phenomenon of lower residual normal displacement.

5. Shear Surface Morphological Characteristics

5.1. 3D Morphological Scan Results

The surface morphology of coal rock joints is closely related to their mechanical properties, so a correct description of the surface morphology of coal rock joints is the only prerequisite for studying the damage characteristics of coal rock bodies.

Combined with the data in **Table 2**, it can be concluded from **Figure 13** that when the normal stress of the coal sample is 0.5 MPa, the undulation of the entire section profile is high, and the maximum height of the fissure surface profile reaches 0.85 as the maximum value, which is a high-order undulating section; secondly, when the normal stress of the coal sample is 1.5 MPa, the undulation of the entire section profile is relatively small, and the maximum height of the fissure surface profile is reduced by 25% compared with the maximum value, which is a low-order undulating section. At a normal stress of 2 MPa, the entire section is generally flat, with a large number of small concave and convex bodies in the section, but no large bumps or depressions, and the maximum height of

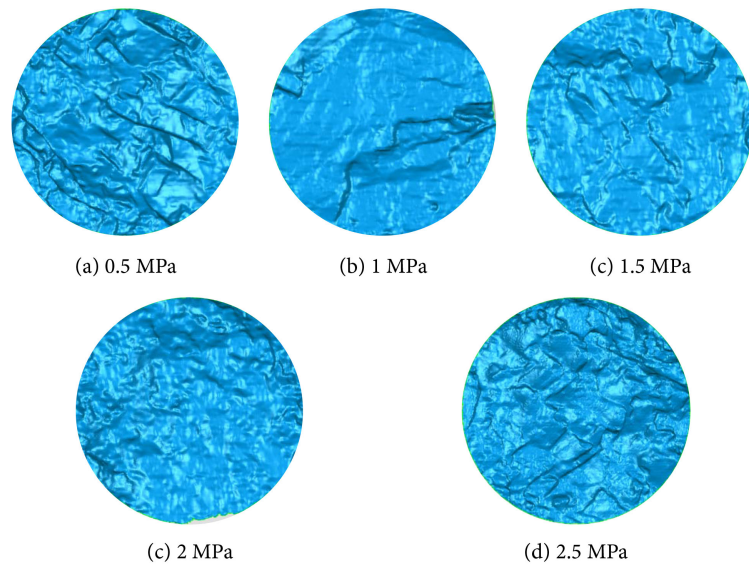


Figure 13. Visualisation of the shear section of a coal sample under different normal stresses.

Table 2. 3D morphological scan results.

σ_n	S_z	S_{ku}	R_s	Z_2
0.5	0.85	5.70	1.25	2.87
1	0.77	4.30	1.17	1.21
1.5	0.64	3.62	1.09	0.97
2	0.23	2.87	1.08	1.06
2.5	0.59	5.22	1.23	2.03

In the table, σ_n is the normal stress, S_z is the maximum height of the fissure face profile, S_{ku} is the kurtosis factor, R_s is the profile area ratio and Z_2 is the root mean square of the slope.

the fracture surface profile reaches a minimum of 0.23, which is a flat type of section. Therefore, it can be seen that as the normal stress increases, the intuitive shape of the shear surface of the coal sample transitions from a higher order undulating type to a flat type, indicating that the higher the normal stress, the more the main projection of the shear surface of the specimen is restricted in its climbing shear expansion behaviour, and the main projection of the shear surface is more likely to undergo tooth-cutting damage and be sheared off from the root, resulting in a flatter section shape.

5.2. Discrete Analysis

The three-dimensional morphological parameters of the coal sample under 2.5 MPa normal stress are obviously discrete. Wang Wei [1] concluded that the anisotropy of the sandstone does not fundamentally change the morphological information of the shear section by analysing the three-dimensional morphological characteristics of the sandstone shear section under different normal

stresses. **Figure 14** shows the shear section of a coal sample at 2.5 MPa normal stress, from which it can be seen that there are a large number of laminations and joints within the sample, the presence of which not only affects the shear behaviour, but also has a different degree of influence on the morphological parameters of the sample. Combined with **Figure 6** and **Figure 9**, it can be seen that compared to the other four specimens, the 2.5 MPa normal stress coal sample did not have a sudden drop in stress near the peak shear strength as the other four samples, which may be due to the fact that after the initial shearing, the roughness of the section morphology formed by the presence of laminae and joints was relatively high and still provided part of the shear strength; the 2.5 MPa normal stress coal sample had a higher shear strength compared to the the 2.5 MPa normal stress coal sample was more pronounced than the other four specimens in that the normal shear expansion followed by normal shear contraction occurred in the section. This may be due to the influence of the complex laminae and joints within the coal sample when shearing occurred.

In summary, due to the obvious anisotropic nature of the 2.5 MPa normal stress coal samples, the 2.5 MPa normal stress coal samples can be excluded from the analysis of the relationship between normal stress and the characteristics of each morphological parameter, so that the regularity of the relationship between normal stress and the four main 3D morphological parameters will be more obvious.

5.3. Relationship between 3D Morphological Parameters and Normal Stress

The maximum height of the fracture surface profile (S_z) refers to the absolute value of the distance between the highest point of the peak curve of the fracture surface profile and the lowest point of the valley curve of the fracture surface profile within the sampling area, the larger this value is the greater the undulation of the fracture surface. As can be seen from **Figure 15**, the maximum height of the fissure surface profile and the normal stress are linearly decreasing, when the normal stress is small, the creeping effect of the shear surface is more obvious, when the normal stress is larger, the creeping effect of the shear surface is limited, and the damage form of the bulge is gradually transitioned from tip damage to central shear and root shear.



Figure 14. 2.5 MPa normal stress coal sample shear section.

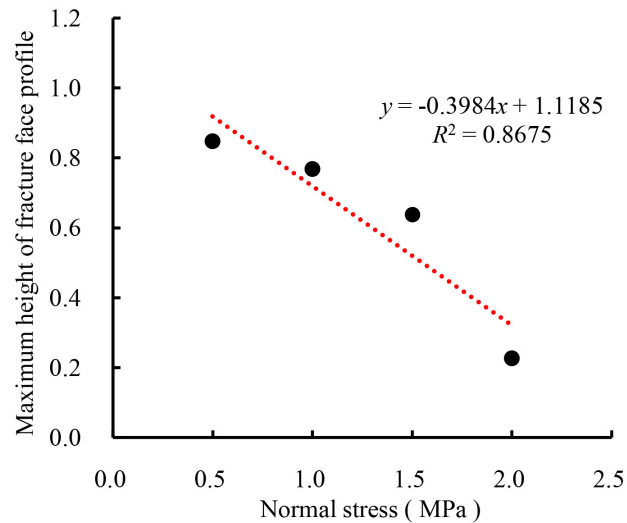


Figure 15. Relationship between maximum height of fracture surface profile and normal stress.

The value of the contour area ratio R_s can reflect the roughness of the fracture surface, the greater the absolute value of its value deviation from 1, the rougher the fracture surface, and conversely, the smoother the fracture surface. It can be seen from **Figure 16** that the contour area ratio decreases as a power function with the increase in normal stress and gradually approaches 1.

The peak coefficient S_{ku} can reflect the concentration degree of the distribution probability of crack surface height, and the roughness shape sharpness can be judged by its value. The S_{ku} value is 3 as the dividing line. $S_{ku} < 3$ indicates that the height distribution of the fractured surface is relatively discrete, that is, the roughness shape of the fractured surface is relatively flat. $S_{ku} > 3$ indicates that the height distribution of the crack surface is concentrated, that is, the roughness shape of the crack surface is sharp. As can be seen from **Figure 17**, with the increase of normal stress, the height distribution of shear section of coal sample transitions from centralized to discrete, that is, the larger the normal stress is, the smoother the joint surface morphology will be.

The root mean square of slope decreases as a power function with the increase of normal stress. The correlation coefficient between slope root-mean-square Z_2 and JRC is the highest compared with the other three 3D morphologic features [22] [23], and the relationship between the two is as follows:

$$JRC_{2D} = 32.69 + 32.98 \log_{10} Z_2 \quad (1)$$

Its value is positively correlated with the fracture surface roughness coefficient JRC , so the root mean square of the slope can be used to reflect the trend of the shear surface roughness coefficient JRC with the normal stress. From **Figure 18**, it can be concluded that the higher the normal stress, the smaller the root mean square of the shear surface slope Z_2 , and the lower its positively correlated roughness coefficient JRC , the smoother the shear surface.

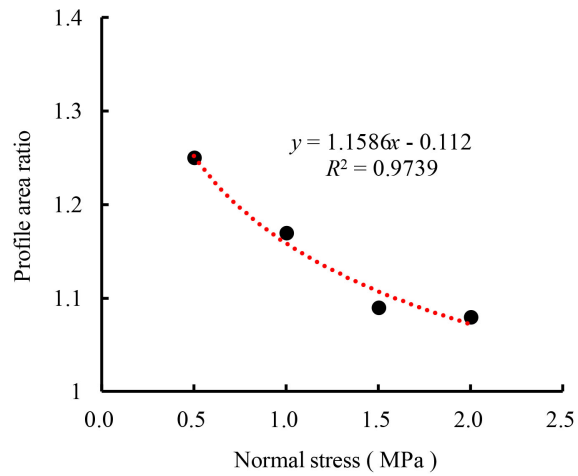


Figure 16. Relationship between profile area ratio and normal stress.

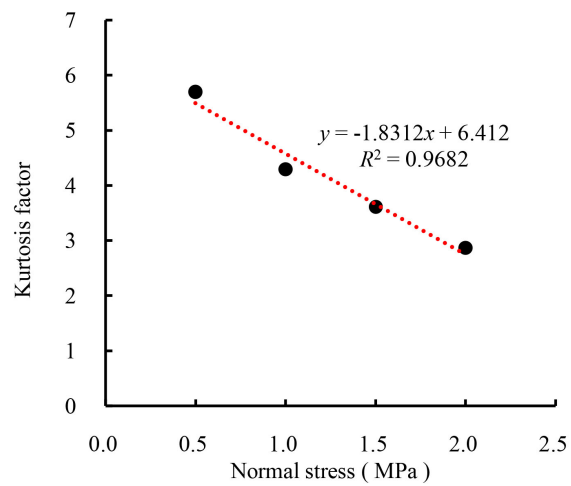


Figure 17. Relationship between kurtosis factor and normal stress.

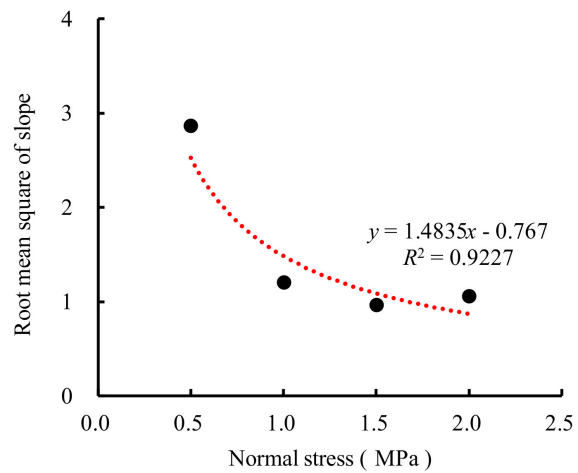


Figure 18. Relationship between the root mean square of the slope and the normal stress.

6. Conclusions

In this paper, by carrying out straight shear tests and shear surface scans of coal samples under different normal stresses, the following main conclusions were drawn:

1) Based on the characteristics of the shear stress-shear displacement curve, the damage of coal samples under shear loading is divided into five stages: compression-density stage, linear stage, yield stage, softening stage and residual stage. The peak shear strength of the coal sample increases linearly with increasing normal stress, and the residual shear strength of the coal sample increases logarithmically with increasing normal stress.

2) The normal stress has a limiting effect on the shear swelling effect in the section. At low normal stresses, the deformation of the shear section is characterised by normal shear expansion; at high normal stresses, it is characterised by normal shear contraction.

3) The higher the normal stress, the greater the peak shear displacement of the coal sample increases linearly, the residual normal displacement decreases linearly and the peak front shear stiffness increases logarithmically.

4) The higher the normal stress, the higher the normal stress, the more the shear surface transition from a higher order undulating profile to a flat profile. As the normal stress increases, the maximum height of the fracture surface profile and the kurtosis coefficient of the shear surface decrease linearly, and the area ratio of the profile and the root mean square of the slope decrease as a power function, *i.e.* the higher the normal stress, the lower the undulation of the shear surface, the lower the sharpness of the roughness shape, the smaller the shear surface roughness coefficient JRC value, and the flatter and smoother the section.

Conflicts of Interest

The authors declare no conflicts of interest regarding the publication of this paper.

References

- [1] Wang, W. (2019) Experimental Study on the Mechanical Properties of Coal Rocks Under Shear-Percolation Coupling and the Morphological Characteristics of Their Shear Surfaces. Chongqing University, Chongqing. (In Chinese)
- [2] Zhao, K. (2020) Three-Dimensional Morphological Characteristics and Shear Mechanical Properties of the Structural Surface of the Coal Body Laminae. General Research Institute of Coal Science, Beijing.
- [3] Li, P., Liu, J., Zhu, J.B., *et al.* (2008) Study on the Relationship between Shear Creep Properties and Water Content of Soft Structural Surfaces. *Rock and Soil Mechanics*, No. 7, 1865-1871. (In Chinese)
- [4] Li, H.B., Feng, H.P. and Liu, B. (2006) Study on Strength Behaviors of Rock Joints under Different Shearing Deformation Velocities. *Chinese Journal of Rock Mechanics and Engineering*, **12**, 2435-2440. (In Chinese)

- [5] Wang, J., He, M. and Wang, Z.W. (2006) Relationship between the Shear Strength and Water Content of Swelling Sandstones. *China Civil Engineering Journal*, **39**, 98-102. (In Chinese)
- [6] Xiao, F.K., Hou, Z.Y., He, J. and Liu, G. (2018) Mechanical Characteristics and Acoustic Emission Characteristics of Coal Samples under Variable Angle Shear. *Journal of China University of Mining and Technology*, **47**, 822-829. (In Chinese)
- [7] Peng, S.J., Xu, J., Zhang, C.L., Feng, D. and Nie, W. (2015) Fractal Characteristics of Crack Evolution in Gas-Bearing Coal Under Shear Loading. *Journal of China Coal Society*, **40**, 801-808. (In Chinese)
- [8] Xu, J., Wang, W., Liu, Y.X., *et al.* (2018) Experimental Study on Shear-Seepage for Coal-Rock Shear Fracture Surface Morphological Characteristics. *Rock and Soil Mechanics*, **39**, 4313-4324+4334. (In Chinese)
- [9] Wang, G., Zhang, X.P., Jiang, Y.J. and Zhang, Y.Z. (2015) New Shear Strength Criterion for Rough Rock Joints Considering Shear Velocity. *Chinese Journal of Geotechnical Engineering*, **37**, 1399-1404. (In Chinese)
- [10] Li, W.F., Bai, J.B. Cheng, J.Y., Peng, S. and Liu, H.L. (2015) Determination of Coal-Rock Interface Strength by Laboratory Direct Shear Tests under Constant Normal Load. *International Journal of Rock Mechanics and Mining Sciences*, **77**, 60-67. <https://doi.org/10.1016/j.ijrmms.2015.03.033>
- [11] Xu, J., Liu, Y.X., Tan, H. and Zhang, H.L. (2016) Three Dimensional Statistical Analysis of Fracture Roughness of Sandstone under Shear Loading. *Journal of Northeastern University (Natural Science Edition)*, **37**, 1034-1039. (In Chinese)
- [12] Xia, C.C., Xiao, W.M., Wang, W. and Ding, Z.Z. (2010) Calculation Method for Three-Dimensional Composite Topography of Joint under Different Contact Conditions. *Chinese Journal of Rock Mechanics and Engineering*, **29**, 2203-2210. (In Chinese)
- [13] Xia, C.C., Wang, W. and Ding, Z.Z. (2008) Development of Three-Dimensional TJXW-3D-Typed Portable Rock Surface Topography. *Chinese Journal of Rock Mechanics and Engineering*, **27**, 1505-1512. (In Chinese)
- [14] Xia, C.C., Tang, Z.C. and Song, Y.L. (2013) A New Peak Shear Strength Formula for Matching Irregular Joints Based on 3D Morphology Parameters. *Chinese Journal of Rock Mechanics and Engineering*, **32**, 2833-2839. (In Chinese)
- [15] Jiang, Z., Cao, P., Fan, X., He, Y. and Fan, W.C. (2014) Evolution of Joint Morphology Subjected to Shear Loads Based on Gaussian Filtering Method. *Journal of Central South University (Science and Technology)*, **45**, 1975-1982. (In Chinese)
- [16] Fan, X., Cao, P. and Jin, J. (2012) Experimental Study of the Evolution of the Surface Roughness of Joints. *Journal of Wuhan University of Technology*, **34**, 117-121. (In Chinese)
- [17] Liu, S.L., Wang, C.S., Du, S.G., *et al.* (2022) 3D Morphology Reconstruction of Rock Joints from 2D Profile Measurement by a Profilograph. *Measurement*, **203**, Article ID: 112008. <https://doi.org/10.1016/j.measurement.2022.112008>
- [18] Huang, M., Hong, C.J., Sha, P., *et al.* (2023) Method for Visualizing the Shear Process of Rock Joints Using 3D Laser Scanning and 3D Printing Techniques. *Journal of Rock Mechanics and Geotechnical Engineering*, **15**, 204-215. <https://doi.org/10.1016/j.jrmge.2022.02.013>
- [19] Barton, N. (1982) Modelling Rock Joint Behavior from in Situ Block Tests: Implications for Nuclear Waste Repository Design. Terra Tek, Inc., Salt Lake City.
- [20] Wibowo, J. (1994) Effect of Boundary Conditions and Surface Damage on the Shear

Behavior of Rock Joints: Tests and Analytical Predictions. University of Colorado, Colorado.

- [21] Asadollahi, P. (2009) Stability Analysis of a Single Three Dimensional Rock Block: Effect of Dilatancy and High-Velocity Water Jet Impact. University of Texas at Austin, Texas.
- [22] Li, Y. and Zhang, Y. (2015) Quantitative Estimation of Joint Roughness Coefficient Using Statistical Parameters. *International Journal of Rock Mechanics and Mining Sciences*, **77**, 27-35. <https://doi.org/10.1016/j.ijrmms.2015.03.016>
- [23] Zheng, B. and Qi, S. (2016) A New Index to Describe Joint Roughness Coefficient (JRC) under Cyclic Shear. *Engineering Geology*, **212**, 72-85. <https://doi.org/10.1016/j.enggeo.2016.07.017>